

## Unprecedented Solvent-Assisted Reactivity of Hydrido $W_3CuS_4$ Cubane Clusters: The Non-Innocent Behaviour of the Cluster-Core Unit

Andrés G. Algarra,<sup>[a]</sup> Marta Feliz,<sup>\*[b]</sup> M. Jesús Fernández-Trujillo,<sup>[a]</sup> Rosa Llusar,<sup>\*[b]</sup> Vicent S. Safont,<sup>[b]</sup> Cristian Vicent,<sup>[c]</sup> and Manuel G. Basallote<sup>\*[a]</sup>

**Abstract:** Reaction of the incomplete cuboidal cationic cluster  $[W_3S_4H_3(dmpe)_3]^+$  ( $dmpe = 1,2$ -bis(dimethylphosphino)ethane) with  $Cu^I$  compounds produces rare examples of cationic heterodimetallic hydrido clusters of formula  $[W_3CuClS_4H_3(dmpe)_3]^+$  (**[1]**<sup>+</sup>) and  $[W_3Cu(CH_3CN)S_4H_3(dmpe)_3]^{2+}$  (**[2]**<sup>2+</sup>). An unexpected conversion of **[1]**<sup>+</sup> into **[2]**<sup>2+</sup>, which involves substitution of chloride by  $CH_3CN$  at the copper centre, has been observed in  $CH_3CN/H_2O$  mixtures. Surprisingly, formation of the acetonitrile

complex does not occur in neat acetonitrile and requires the presence of water. The kinetics of this reaction has been studied and the results indicate that the process is accelerated when the water concentration increases and is retarded in the presence of added chloride. Computational studies have also been carried out and a mechanism

**Keywords:** cluster compounds · copper · density functional calculations · kinetics · tungsten

for the substitution reaction is proposed in which attack at the copper centre by acetonitrile or water causes disruption of the cubane-type core. ESI-MS experiments support the formation of intermediates with an open-core cluster structure. This kind of process is unprecedented in the chemistry of  $M_3M'Q_4$  ( $M = Mo, W$ ;  $Q = S, Se$ ) clusters, and allows for the transient appearance of a new coordination site at the  $M'$  site which could explain some aspects of the reactivity and catalytic properties of this kind of clusters.

### Introduction

The chemistry of multimetallic sulfido clusters has received much attention owing to its relevance to the active sites of metalloenzymes and industrial metal-sulfide catalysts.<sup>[1–4]</sup> In

the last 20 years, the reactivity and kinetics of ligand-exchange<sup>[5–9]</sup> and isomerisation reactions<sup>[10–12]</sup> at the  $M'$  centres in cuboidal  $M_3M'S_4$  clusters ( $M = Mo, W$ ;  $M' = Fe, Ru, Co, Ni, Pd, Pt, Cu$ ) have been intensely studied. The  $M_3M'S_4$  units remain intact in all cases, thus indicating the robustness of these units. Nevertheless, catalytic reactions and mechanistic studies have been largely unexplored.<sup>[13]</sup> Exceptions to the latter are palladium- and nickel-based  $Mo_3M'S_4$  systems where the molybdenum atoms are coordinated to 1,4,7-triazacyclononane,  $\eta^5$ -pentamethylcyclopentadienido or aquo ligands, which catalyse a variety of processes including the addition of methanol or carboxylic acids to electron-deficient alkynes,<sup>[7]</sup> the intramolecular hydroamination of aminoalkynes,<sup>[14]</sup> the cyclisation of alkynoic acids to enol lactones<sup>[15]</sup> and the hydrodesulfurisation of benzothio-phenes.<sup>[16,17]</sup> Catalytic studies centred on  $Mo_3RuS_4$  clusters have explored their behaviour as effective catalysts for N–N bond cleavage in hydrazines.<sup>[18]</sup>

$M_3CuS_4$  clusters coordinated to diphosphanes have attracted attention because of their catalytic activity in the intra- and intermolecular cyclopropanation of diazo compounds<sup>[19,20]</sup> and their particular non-linear optical properties.<sup>[21]</sup> These clusters are easily accessible by direct incorporation of copper into the homometallic  $M_3(\mu_3-S)(\mu-S)_3$  clus-

[a] A. G. Algarra, Prof. M. J. Fernández-Trujillo, Prof. M. G. Basallote  
Departamento de Ciencia de los Materiales e  
Ingeniería Metalúrgica y Química Inorgánica  
Universidad de Cádiz, Polígono Río San Pedro  
Puerto Real, Cádiz, 11510 Cádiz (Spain)  
Fax: (+34)956-016-288  
E-mail: manuel.basallote@uca.es

[b] Dr. M. Feliz, Prof. R. Llusar, Prof. V. S. Safont  
Department de Química Física i Analítica  
Universitat Jaume I, Av. Sos Baynat  
s/n, 12071 Castelló de la Plana (Spain)  
Fax: (+34)964-728-066  
E-mail: feliz@qfa.uji.es  
llusar@qfa.uji.es

[c] Dr. C. Vicent  
Serveis Centrals d'Instrumentació Científica  
Universitat Jaume I, Av. Sos Baynat  
s/n, 12071 Castelló de la Plana (Spain)

Supporting Information for this article is available on the WWW  
under <http://dx.doi.org/10.1002/chem.200802473>.

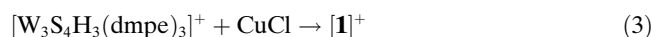
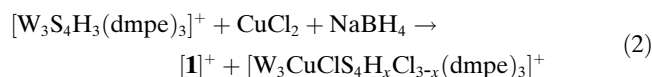
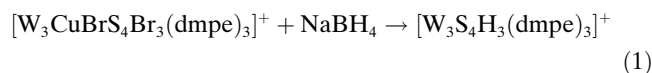
ter framework by binding to the available lone pairs of the bridging sulfur ligands or by displacement of less thiophilic metal atoms. Multidentate ligands, such as diphosphanes,<sup>[19,20]</sup> dithiophosphates,<sup>[22–24]</sup> cyclopentadienidos,<sup>[25]</sup> dithiocarbamates,<sup>[26]</sup> dithiophosphinates or acetates,<sup>[27]</sup> coordinated to the molybdenum or tungsten atoms of the  $M_3S_4$  unit favour the solubility of the  $M_3CuS_4$  products in organic solvents. In all these cases, the copper atom is coordinated to tricapped sulfur ligands and to one water molecule or halogen atom (Cl, Br, I) to complete a pseudotetrahedral geometry.<sup>[8,28]</sup>

Herein we report the synthesis of the cationic hydrido clusters  $[W_3CuClS_4H_3(dmpe)_3]^+$  ( $[1]^+$ ) and  $[W_3Cu(CH_3CN)_4S_4H_3(dmpe)_3]^{2+}$  ( $[2]^{2+}$ ), where each of the tungsten atoms has a coordinated hydride. These compounds represent the second examples of heterobimetallic hydride  $M_3M'S_4$  clusters after  $[W_3Pd(CO)S_4H_3(dmpe)_3]^+$ .<sup>[29]</sup> The high stability of  $[1]^+$ , and its solubility in a wide variety of solvents, makes it a potentially excellent substrate for investigating the mechanism of protonation of hydride complexes. Thus, the terminal hydrides in  $[W_3Q_4H_3(dmpe)_3]^+$  ( $Q=S, Se$ ) and  $[W_3Pd(CO)S_4H_3(dmpe)_3]^+$  have previously been shown to undergo acid-promoted substitution reactions through the formation of dihydrogen-bonded adducts, with the reaction kinetics and mechanism showing a strong dependence on the coordinating capability of the solvent.<sup>[29–32]</sup> The results reported herein indicate that cluster  $[1]^+$  is not as stable as  $[W_3Pd(CO)S_4H_3(dmpe)_3]^+$  in acidic media, and products resulting from cluster core degradation are obtained upon reaction with acids. During the course of this work a very interesting and unexpected conversion of cluster  $[1]^+$  into  $[2]^{2+}$  was observed in  $CH_3CN/H_2O$  mixtures, with formation of the acetonitrile complex  $[2]^{2+}$  from  $[1]^+$  being promoted by water. From a qualitative point of view, this reaction can be considered a new example of a process driven by solvation of the released chloride,<sup>[33–35]</sup> and a detailed experimental and theoretical study has been carried out with the aim of elucidating the kinetic and mechanistic features of this process. These studies have revealed an active role of the cluster core on the reactivity of the heterometal site, which is unprecedented in the chemistry of these compounds and opens up new possibilities for a better understanding of certain aspects of the reactivity and catalytic properties of this kind of clusters.

## Results and Discussion

**Synthesis and structure:** Trinuclear  $M_3(\mu_3-S)(\mu-S)_3$  ( $M=Mo, W$ ) cubane-type clusters have been widely used as metallo-ligands towards other transition metals to produce a large variety of heterobimetallic  $M_3M'(\mu_3-S)_4$  complexes by the so-called [3 + 1] building block approach.<sup>[36–38]</sup> We have previously reported that the cationic cluster  $[W_3CuBrS_4Br_3(dmpe)_3]^+$  can be obtained from the reaction between  $[W_3S_4Br_3(dmpe)_3]^+$  and  $[Cu(CH_3CN)_4]^+$  in the presence of  $(\mu-Bu_4N)Br$ , or between  $[W_3S_4Br_3(dmpe)_3]^+$  and  $CuBr$ , in

moderate yields (58% and 37%, respectively).<sup>[21]</sup> In the present work, we have explored different synthetic routes to access cubane-type  $W_3CuS_4$  hydrides [Equations (1–4)].



Synthesis of  $W_3CuS_4$  hydrides was attempted by treating the all-bromine cluster  $[W_3CuBrS_4Br_3(dmpe)_3]PF_6$  with  $NaBH_4$  in THF [Eq. (1)]; however, the trinuclear cationic complex  $[W_3S_4H_3(dmpe)_3]^+$  was the only characterisable product, as judged by ESI mass spectrometry and  $^{31}P\{^1H\}$  and  $^1H$  NMR spectroscopy. Addition of a DMF solution of  $CuCl_2$  to a suspension of  $[W_3S_4H_3(dmpe)_3]PF_6$  and  $NaBH_4$  in THF, as represented in [Eq. (2)], gives  $[1]^+$  together with  $[W_3CuClS_4H_xCl_{3-x}(dmpe)_3]^+$  species, which were identified by ESI mass spectrometry and NMR spectroscopy. Finally,  $[W_3S_4H_3(dmpe)_3]PF_6$  reacts with  $CuCl$  [Eq. (3)] or  $[Cu(CH_3CN)_4]PF_6$  [Eq. (4)] to give  $[W_3CuS_4H_3Cl(dmpe)_3]PF_6$  ( $[1]PF_6$ ) and  $[W_3CuS_4H_3(dmpe)_3(CH_3CN)](PF_6)_2$  ( $[2](PF_6)_2$ ), respectively, in good yield (ca. 90%). Compounds  $[1]PF_6$  and  $[2](PF_6)_2$  were characterised by ESI mass spectrometry and IR and  $^{31}P\{^1H\}$ ,  $^{13}C$  and  $^1H$  NMR spectroscopy (see Experimental Section). Cluster  $[2]^{2+}$  decomposes in solution in air (ca. 20% after 24 h) to give  $[W_3S_4H_x(OH)_{3-x}(dmpe)_3]^+$  and copper salts, which were identified by ESI mass spectrometry and NMR spectroscopy.

Crystals of compound  $[1]PF_6$  suitable for X-ray analysis were obtained.  $[1]PF_6$  crystallises in the hexagonal space group  $P6_3$ , and the intermetallic W–W distances are indicative of a  $C_3$  symmetry, in agreement with the presence of two different resonance signals in the  $^{31}P\{^1H\}$  NMR spectra. Figure 1 shows an ORTEP drawing of the  $[1]^+$  cluster cation together with the atom numbering scheme.

The metal cluster core consists of a slightly distorted tetrahedral arrangement of one copper and three tungsten atoms. Each tetrahedral face is capped by a  $\mu_3$ -coordinated sulfide ligand to generate a cubane-like structure. The coordination sphere around each tungsten atom is essentially octahedral, with each W(1) site coordinated to two phosphorus atoms [P(1) and P(2)] located *trans* to  $\mu_3$ -S(1) and  $\mu_2$ -S(2), respectively, and a vacant position associated with the hydride ligand *trans* to the other  $\mu_2$ -S(2) bridging ligand. The existence of three hydride ligands, one on each W atom, was fully supported by  $^1H$  and  $^{31}P$  NMR spectroscopy. The tetrahedral environment around Cu(1) is defined by three bridging sulfur atoms and one chlorine ligand. Table 1 shows the most relevant bond distances within the cluster unit in  $[1]PF_6$  together with those found for its halogenated analogue  $[W_3CuBrS_4Br_3(dmpe)_3]^+$ .

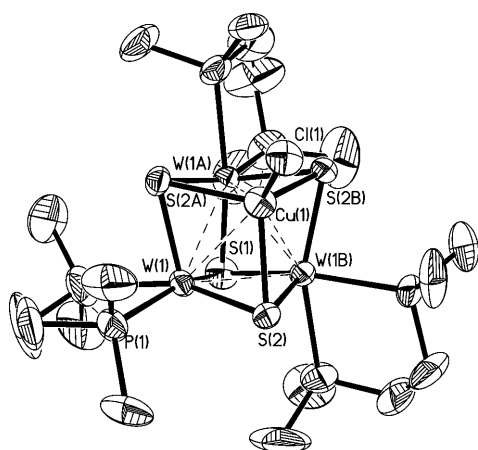


Figure 1. ORTEP representation of cation  $[1]^+$ . Hydrogen atoms have been omitted for clarity.

Table 1. Selected average bond distances [ $\text{\AA}$ ] for  $[1]\text{PF}_6$  and  $[\text{W}_3\text{CuBrS}_4\text{Br}_3(\text{dmpe})_3]\text{PF}_6$ .<sup>[a]</sup>

Dist. [ $\text{\AA}$ ]	$[1]\text{PF}_6$	$[\text{W}_3\text{CuBrS}_4\text{Br}_3(\text{dmpe})_3]\text{PF}_6$ <sup>[21]</sup>
W–W	2.7620(6)	2.780 <sup>[2]</sup>
W–Cu	2.851(2)	2.884 <sup>[7]</sup>
W– $\mu_3$ -S(1)	2.368(3)	2.363 <sup>[2]</sup>
W– $\mu_3$ -S(2) <sup>[b]</sup>	2.367(2)	2.331 <sup>[5]</sup>
W– $\mu_3$ -S(2) <sup>[c]</sup>	2.371(2)	2.365 <sup>[5]</sup>
Cu– $\mu_3$ -S(2)	2.380(2)	2.320 <sup>[13]</sup>
W–X	–	2.627 <sup>[12]</sup>
Cu–X	2.209(4)	2.303(2)

[a] Standard deviations for average values are given in brackets. X corresponds to a hydride or bromine atom. [b] W–S–(W,Cu) *trans* distance to W–X bond. [c] W–S–(W,Cu) *trans* distance to Mo–P(2) bond.

Cation  $[1]^+$  shares structural features with its brominated  $\text{W}_3\text{Cu}$  analogue  $[\text{W}_3\text{CuBrS}_4\text{Br}_3(\text{dmpe})_3]^+$ . The average W–W and W–Cu bond distances of 2.7620(6) and 2.851(2)  $\text{\AA}$ , respectively, are consistent with the presence of single bonds between metal atoms. The most significant structural variation on going from  $[1]^+$  to  $[\text{W}_3\text{CuBrS}_4\text{Br}_3(\text{dmpe})_3]^+$  concerns the intra-cluster Cu–S bonds.<sup>[21]</sup>

**Kinetic studies on the reactivity of cluster  $[1]^+$ :** Reactivity and kinetic studies have shown that cluster  $[1]^+$  is stable in neat acetonitrile solutions, even in the presence of acids such as HCl (see the Supporting Information). However, addition of water changes the stability of this compound. Thus, kinetic experiments have shown that the reaction between  $[1]^+$  and HCl in  $\text{CH}_3\text{CN}/\text{H}_2\text{O}$  solution gives mainly  $[\text{W}_3\text{S}_4\text{Cl}_3(\text{dmpe})_3]^+$  and  $[2]^+$  (see the Supporting Information). Furthermore, a clean and unexpected conversion of  $[1]^+$  to  $[2]^{2+}$  occurs when water is added to an acetonitrile solution of  $[1]^+$  (see Eq. (5) below). Even though water does not appear explicitly in Equation (5), its presence is required to drive the reaction to the right-hand side.  $^{31}\text{P}\{^1\text{H}\}$  NMR experiments (Figure 2) clearly show that it is possible to observe the progressive conversion of  $[1]^+$  (signals at  $\delta = 6.66$  and  $-5.25$  ppm) to  $[2]^{2+}$  (signals at  $\delta = 5.69$  and  $-3.86$  ppm) by adding different aliquots of  $\text{H}_2\text{O}$  to an NMR

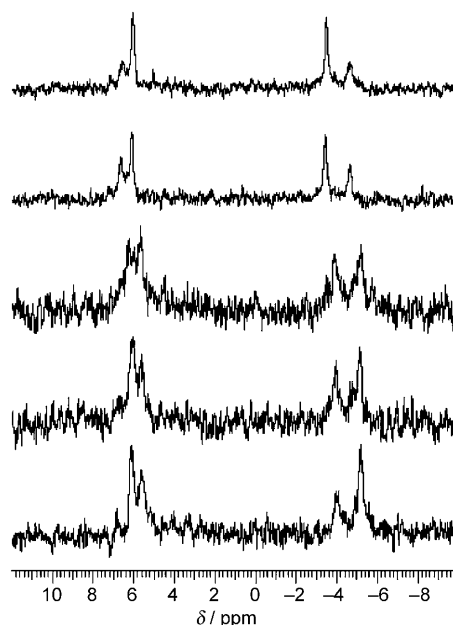


Figure 2.  $^{31}\text{P}\{^1\text{H}\}$  NMR spectra obtained after sequential addition of  $\text{H}_2\text{O}$  aliquots to a sample of  $[1]^+$  (ca. 0.01 M) in acetonitrile. The successive spectra starting from the bottom show the gradual conversion of  $[1]^+$  into  $[2]^+$  as the water content increases. The  $\text{H}_2\text{O}/\text{CH}_3\text{CN}$  ratio for the different spectra is 0.15, 0.20, 0.25, 0.33 and 0.45.

tube containing a concentrated solution of  $[1]^+$  in acetonitrile. These experiments also reveal that the process occurs without accumulation of any other product detectable by  $^{31}\text{P}\{^1\text{H}\}$  NMR spectroscopy. The formation of  $[2]^{2+}$  (and not the related aquo complex) as the reaction product is further supported by ESI mass spectrometry—the mass spectrum observed after  $\text{H}_2\text{O}$  addition to an acetonitrile solution of  $[1]^+$  coincides with that obtained for solutions prepared from a sample of authentic  $[2]^{2+}$  and neat acetonitrile. The most intense signal appears at  $m/z$  618.5 and corresponds to the dicationic cluster  $[\text{W}_3\text{Cu}(\text{CH}_3\text{CN})\text{S}_4\text{H}_3(\text{dmpe})_3]^{2+}$ .



It is important to note the essential role of water in promoting the reaction in Equation (5) despite the fact that water addition is inevitably accompanied by a decrease in the acetonitrile concentration in the resulting mixed solvent. The NMR and ESI-MS experiments described above clearly indicate that water causes the thermodynamics of the process to change, an effect whose origin can be qualitatively attributed to preferential solvation of the released  $\text{Cl}^-$  ion by water acting as the driving force for the process. There are several examples of inorganic and organic reactions in which a similar effect has been observed.<sup>[33–35]</sup> The free energy for transfer of this anion from acetonitrile to water is  $-10.1 \text{ kcal mol}^{-1}$ , and intermediate values have been measured for  $\text{CH}_3\text{CN}/\text{H}_2\text{O}$  mixtures of different compositions.<sup>[39,40]</sup> Thus, the solvation changes associated with the presence of significant amounts of water favour the formation of the acetonitrile complex (by a few  $\text{kcal mol}^{-1}$ ). How-

ever, the process represented in Equation (5) is more complex as there is also a change in the charge of the cluster, which must necessarily lead to additional significant solvation changes. Moreover, the possibility of water also having a kinetic effect by acting as an entering ligand cannot be ruled out. Although the NMR experiments indicate that no significant amounts of any intermediate are formed, formation of small amounts of an aquo complex as reaction intermediate under steady-state conditions could provide a reaction pathway of lower energy than that involving direct substitution of chloride by acetonitrile. To gain insight into these important aspects, a detailed kinetic and density functional theory (DFT) study of this process was carried out (see below).

The kinetics of the reaction in Equation (5) was studied by mixing an acetonitrile solution of cluster [1]<sup>+</sup> with mixtures of acetonitrile and water in the stopped-flow instrument so that the CH<sub>3</sub>CN/H<sub>2</sub>O ratio in the resulting solution varied between approximately 1:1 and 9:1 (v/v). The experiments were carried out at 25.0°C in the presence of 0.1 M Et<sub>4</sub>NBF<sub>4</sub> and some experiments were also performed in which the cluster concentration was changed for a given composition of the mixed solvent. A typical example of the spectral change with time is depicted in Figure 3, which

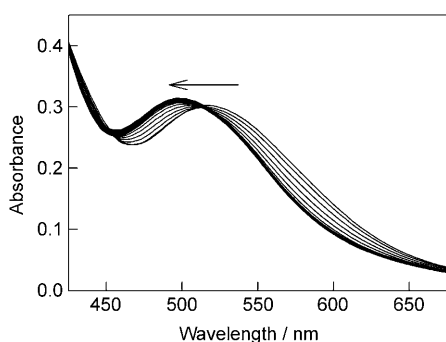


Figure 3. Typical spectral changes with time for the reaction of an acetonitrile solution of [1]<sup>+</sup> with H<sub>2</sub>O (1:1, v/v) at 25°C.

shows that conversion of [1]<sup>+</sup> into [2]<sup>2+</sup> is accompanied by a shift of the absorption band from 516 to 502 nm. These experimental data can be satisfactorily fitted by using a single-step kinetic model—the values derived for the observed rate constant ( $k_{\text{obs}}$ ) are independent of the cluster concentration, which indicates that the process has a first-order dependence with respect to [1]<sup>+</sup>.

The dependence of  $k_{\text{obs}}$  with water concentration is illustrated in Figure 4. The data can be satisfactorily fitted by a linear dependence [Eq. (6), with  $k_a = 0.022 \pm 0.002 \text{ M}^{-1} \text{ s}^{-1}$  and  $k_b = 0.06 \pm 0.03 \text{ s}^{-1}$ ], although a slightly better fit is obtained with a saturation curve [Eq. (7), with  $k_c = 2.0 \pm 0.3 \text{ s}^{-1}$  and  $k_d = (1.8 \pm 0.4) \times 10^{-2} \text{ M}^{-1}$ ]. The medium effects in these experiments are expected to be large given the extremely large water concentrations required to drive the reaction in Equation (5) towards product formation, so the choice between the two fits is always debatable. Furthermore, the

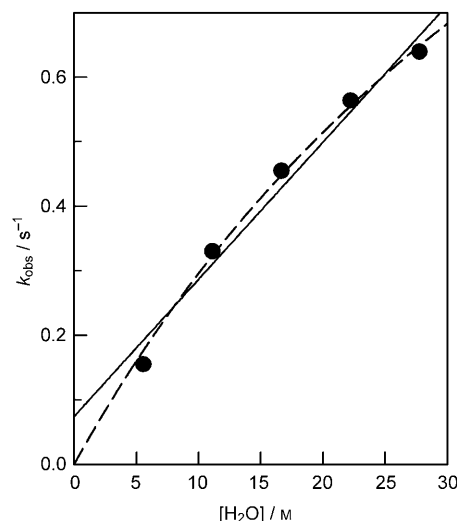


Figure 4. Plot of the observed rate constant versus [H<sub>2</sub>O] for the reaction of [1]<sup>+</sup> with acetonitrile (25°C, 0.1 M Et<sub>4</sub>NBF<sub>4</sub>). The lines correspond to the best fit of the data using Equations (6) (solid) and (7) (dashed).

possibility that changes in Figure 4 (an increase in the rate constant by a factor of about 4 for a fivefold change in the water content) arise exclusively from changes due to solvent composition cannot be fully ruled out. In any case, irrespective of the equation used to fit the data, the kinetic experiments clearly indicate that water not only affects the thermodynamics of Equation (5), but also accelerates the kinetics of the process.

The effect of added Cl<sup>-</sup> ion on the kinetics of the reaction was examined by carrying out experiments in which the chloride concentration was changed while maintaining a fixed acetonitrile/water ratio. Figure 5 shows the results for experiments at acetonitrile/water ratios of 1:1 and 7:3 (v/v), and reveals a substantial decrease in the  $k_{\text{obs}}$  values when the chloride concentration is increased. These experimental results can be satisfactorily fitted by using Equation (8) or its corresponding linear form [Eq. (9)]; the values derived for the kinetic parameters are  $a = 0.77 \pm 0.01 \text{ s}^{-1}$  and  $b = 9.6 \pm 0.4 \text{ M}^{-1}$  for the 1:1 ratio, and  $a = 0.53 \pm 0.02 \text{ s}^{-1}$  and  $b = 20 \pm 3 \text{ M}^{-1}$  for the 7:3 ratio. No reaction is observed upon addition of small amounts of chloride ion (ca. 0.015 M) when the experiment is carried out with a 9:1 (v/v) acetonitrile/water ratio. As expected, the  $a$  values agree well with the  $k_{\text{obs}}$  values in the absence of added chloride. The value of  $b$  differs by a factor of two between both sets of experiments in Figure 5, but it is again not possible to determine how much of this change is owed to a change in the concentrations of the solvents appearing in the rate law and how much is owed to a medium effect associated with the change in solvent composition.

$$k_{\text{obs}} = k_a[\text{H}_2\text{O}] + k_b \quad (6)$$

$$k_{\text{obs}} = \frac{k_c k_d [\text{H}_2\text{O}]}{1 + k_d [\text{H}_2\text{O}]} \quad (7)$$

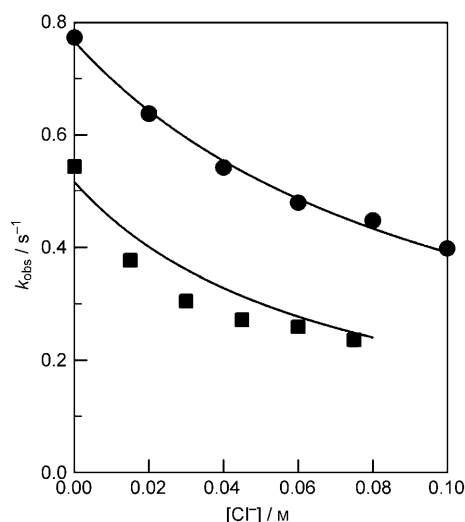
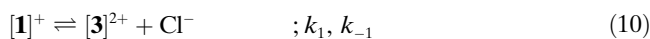


Figure 5. Plots of the observed rate constant versus  $[Cl^-]$  for the reaction of  $[1]^+$  with acetonitrile in acetonitrile/water mixtures (25.0 °C, 0.1 M  $Et_4NBF_4$ ). The experiments marked with (●) were carried out in 1:1 (v/v) acetonitrile/water, while the experiments carried out in 7:3 (v/v) acetonitrile/water are marked with (■). The solid line corresponds to the overall fit of each set of data using Equation (8) with the values of  $a$  and  $b$  given in the text.

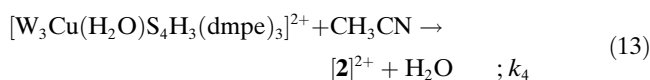
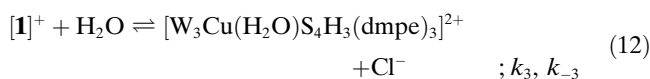
$$k_{\text{obs}} = \frac{a}{1 + b[Cl^-]} \quad (8)$$

$$\frac{1}{k_{\text{obs}}} = \frac{1}{a} + \frac{b}{a}[Cl^-] \quad (9)$$

The observed decrease in  $k_{\text{obs}}$  upon chloride addition provides very important mechanistic information. As the chloride concentrations used in the experiments are relatively low and the dielectric constants of the solvents are quite high, the possibility of the rate inhibition being owed to the formation of less reactive ( $[1]Cl$ ) ion pairs can reasonably be ruled out, therefore the deceleration observed clearly indicates that chloride is released prior to the rate-determining step.<sup>[41]</sup> The simplest interpretation is to consider that the reaction in Equation (5) goes through a dissociative mechanism to give  $[W_3CuS_4H_3(dmpe)_3]^{2+}$  ( $[3]^{2+}$ ), as shown in Equations (10) and (11). The rate law for this mechanism coincides with the experimental one in Equation (8) with the equivalencies  $a = k_1$  and  $b = k_{-1}/k_2[CH_3CN]$ . In this case, the  $a$  values correspond to the rate constant for  $Cl^-$  ion dissociation from the starting complex, and their changes with water concentration should be ascribed exclusively to medium effects caused by the change in the solvent composition. In other words, the experimental data appear to show that chloride dissociation is accelerated when the water content is increased. The  $b$  values represent the discriminating power of the coordinatively unsaturated intermediate, although their change with solvent composition is difficult to rationalize because they are the result of different contributions. In any case, the changes in the experimental values of both parameters are not very large and it can be reasonably accepted that they arise from solvent effects.



However, there is also the possibility that the reaction goes through a reaction intermediate such as  $[W_3Cu(H_2O)S_4H_3(dmpe)_3]^{2+}$ , which would result from substitution of  $Cl^-$  ion by water [Eqs. (12) and (13)]. The rate law for this mechanism is mathematically equivalent to the previous one, although it differs with respect to the definition of the  $a$  and  $b$  parameters:  $a = k_3[H_2O]$  and  $b = k_{-3}/k_4[CH_3CN]$ .



**Theoretical studies:** To obtain a deeper insight into the process leading from  $[1]^+$  to  $[2]^{2+}$ , a theoretical study of this reaction was carried out using DFT procedures with the aim of unravelling the details of the process from both a thermodynamic and a mechanistic point of view. To simplify the discussion of the DFT results, they will be presented in such a way that thermodynamic aspects are discussed first and then the several mechanistic possibilities are commented and related to the experimental findings. Detailed data in both solvents are provided as Supporting Information, but to achieve a clearer presentation of the conclusions the energies in solution are discussed in the text in terms of the average values of the energies obtained in both solvents, which can be considered a reasonable approximation to the values corresponding to solutions in 1/1  $CH_3CN/H_2O$  mixtures.<sup>[42]</sup>

**Thermodynamics:** The gas-phase energy change on going from  $[1]^+ + CH_3CN$  to  $[2]^{2+} + Cl^-$  is calculated to be 140.88 kcal mol<sup>-1</sup>, thus showing it is a very unfavourable process, as expected from the fact that the reaction in Equation (5) begins with a monocation and a neutral species and ends up with a dication and a mononegative anion. Such a charge separation needs a driving force to make the process thermodynamically favourable. The solvent can play this role and, the energy difference between reactants and products is greatly reduced to 18.1 kcal mol<sup>-1</sup> in acetonitrile, and further reduced to 8.0 kcal mol<sup>-1</sup> in water. Thus, the DFT results indicate that there is a clear thermodynamic medium effect of water favouring the process such that substitution is 10 kcal mol<sup>-1</sup> more favoured in water than in acetonitrile, which is qualitatively in agreement with the experimental observations. Furthermore, we have calculated the solvation free energies of  $[1]^+$  (1.86 and -8.15 kcal mol<sup>-1</sup> in acetonitrile and water, respectively)  $[2]^{2+}$  (-55.26 and -67.06 kcal mol<sup>-1</sup> in acetonitrile and water, respectively),  $CH_3CN$  (-0.84 and -3.39 kcal mol<sup>-1</sup> in acetonitrile and water, respectively) and chloride ion (-67.66 and -78.95 kcal mol<sup>-1</sup> in acetonitrile and water, re-

spectively), which indicates that the promoting effect of water is essentially caused by the preferential solvation of Cl<sup>-</sup> ion in water because the changes for all the other species compensate. It is also worth noting that no relevant changes are observed between gas-phase and PCM-calculated geometries. The structures of [1]<sup>+</sup> and [2]<sup>2+</sup> optimised in the gas phase are shown in Figure 6.

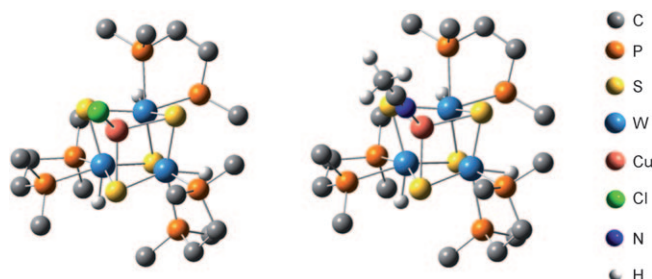


Figure 6. Gas-phase-optimised structures of clusters [1]<sup>+</sup> and [2]<sup>2+</sup>. The H atoms of the diphosphanes have been omitted for simplicity.

Another point that must be considered is that specific interactions of solvent molecules with the reactants can lead to significant changes in the calculated energies. The chloride anion released during the process is the most hydrophilic species, and discrete interactions between the water molecules and the chloride ion could also act as a driving force for the process. Previous experimental<sup>[39,40]</sup> and DFT<sup>[43,44]</sup> results show that microsolvation of halide anions with water is more favourable than with acetonitrile molecules. For this reason, calculations were also made including an increasing number of water molecules in the theoretical model [Eq. (14) with  $n=0-4$ ]. For the reasons given above, these molecules are considered to interact preferentially with the released chloride, and their positions in the starting reagent ([1 $\cdots n$ H<sub>2</sub>O]<sup>+</sup>) were optimised in the region of the coordinated chloride, so that they can be considered to represent the preferential interactions of chloride with water instead of acetonitrile in a better way than simple PCM calculations. The corresponding optimised geometries and energies are given in the Supporting Information. Relative energies to [1]<sup>+</sup> +  $n$ H<sub>2</sub>O are listed in Table 2. The results of calculations considering specific interactions with an increasing number of water molecules are illustrated in Figure 7, which clearly shows that the energy cost for the process in Equation (14) decreases significantly as a larger number of water molecules are included in the model. Extrapolation of the results

Table 2. Reaction energies [kcal mol<sup>-1</sup>] relative to [1]<sup>+</sup> +  $n$ H<sub>2</sub>O + CH<sub>3</sub>CN calculated in CH<sub>3</sub>CN/H<sub>2</sub>O (1:1).

$n$	[1 $\cdots n$ H <sub>2</sub> O] <sup>+</sup> + CH <sub>3</sub> CN	[3] <sup>2+</sup> + [Cl $\cdots n$ H <sub>2</sub> O] <sup>-</sup> + CH <sub>3</sub> CN	[2] <sup>2+</sup> + [Cl $\cdots n$ H <sub>2</sub> O] <sup>-</sup>
0	0.00	41.72	13.06
1	-4.61	34.04	5.38
2	-9.34	27.79	-0.89
3	-12.62	22.33	-6.34
4	-15.86	17.64	-11.03

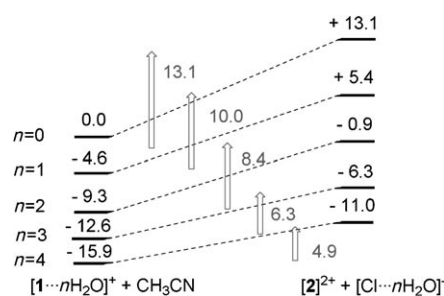
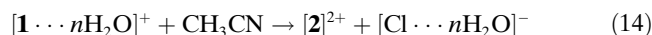
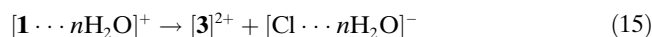


Figure 7. Energies [kcal mol<sup>-1</sup>] in CH<sub>3</sub>CN/H<sub>2</sub>O (1:1) for the reaction in Equation (14).

gives reaction energies close to zero, thus suggesting a thermoneutral character for this process.



**Dissociative mechanism:** Once it had been established that DFT calculations with inclusion of specific interactions with water molecules can explain the displacement of the reaction in Equation (5) to the right-hand side when water is added in a quite satisfactory way, calculations were also made to obtain information about the mechanism of the reaction. A dissociative mechanism with participation of the coordinatively unsaturated species [3]<sup>2+</sup> as reaction intermediate was first considered [Eqs. (15) and (16)]. The release of Cl<sup>-</sup> anion from the starting complex to give [3]<sup>2+</sup> is a very high energy process with a cost of 48.22 kcal mol<sup>-1</sup> in acetonitrile and 35.22 kcal mol<sup>-1</sup> in water (values for  $n=0$ ). These results clearly support that, in addition to the thermodynamic effect commented above, there is a kinetic effect associated with the addition of water which could explain the acceleration observed experimentally as a medium effect. This conclusion is independent of the number of water molecules included in the model, with a slight decrease of the energy barrier of 1–8 kcal mol<sup>-1</sup> being estimated when  $n$  increases (see Figure 8 and Table 2). However, the energy barrier is in all cases too high to explain the experimental values of the reaction rate; that is, the process should be expected to occur significantly more slowly if it were to follow a dissociative mechanism. As this mechanism is also unable to explain the deceleration observed in the presence of added chloride because chloride would not be released before the rate-determining step, alternative reaction pathways had to be explored.



**Mechanisms involving open-core cluster species:** To avoid having to pass through a coordinatively unsaturated intermediate, attempts were made to find more effective associative mechanistic pathways involving coordination of a solvent molecule—either CH<sub>3</sub>CN or H<sub>2</sub>O—to the metal. Two possible mechanisms were envisioned for coordination of

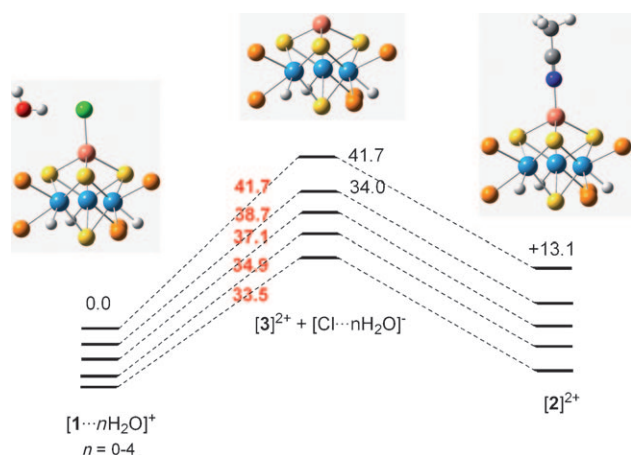
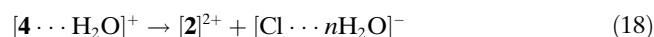
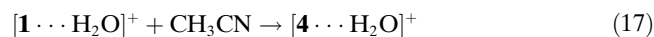


Figure 8. Energy profiles [kcal mol<sup>-1</sup>] obtained for the reaction in Equation (14) in CH<sub>3</sub>CN/H<sub>2</sub>O (1:1) assuming a dissociative mechanism and including a variable number (*n*) of water molecules in the model. In the case of [1···*n*H<sub>2</sub>O]<sup>+</sup>, the geometry shown corresponds to the species with *n*=1.

this solvent molecule. In a first approximation, the associative mechanism represented in Equations (17) and (18), in which the intermediate formulated as [W<sub>3</sub>Cu(Cl···H<sub>2</sub>O)-(CH<sub>3</sub>CN)<sub>4</sub>H<sub>3</sub>(dmpe)<sub>3</sub>]<sup>+</sup> ([4···H<sub>2</sub>O]<sup>+</sup>) is formed before conversion to the final product, was considered. Only one water molecule is included in the model for simplicity, although, as stated above, the participation of more solvent molecules in the real system is evident. The energetic reaction profile is shown schematically in Figure 9.



The acetonitrile molecule enters the coordination sphere of the copper atom with a low energy barrier (1.9 kcal mol<sup>-1</sup>) to give [4···H<sub>2</sub>O]<sup>+</sup> as a stable reaction intermediate (-4.5 kcal mol<sup>-1</sup>). The second reaction step, which has a higher activation barrier of 10.8 kcal mol<sup>-1</sup>, involves bond dissociation between the hydrated chloride and Cu atoms to give [2]<sup>2+</sup> and an energy release of around 1 kcal mol<sup>-1</sup>.

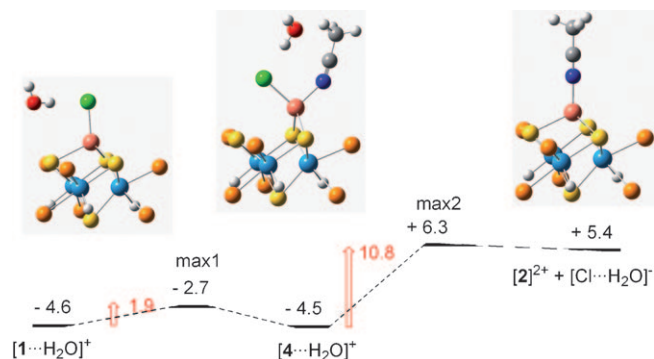


Figure 9. Energy profile [kcal mol<sup>-1</sup>] in CH<sub>3</sub>CN/H<sub>2</sub>O (1:1) for the mechanism represented in Equations (17) and (18).

These results were unexpected because the coordination number around the copper atom in species [4···H<sub>2</sub>O]<sup>+</sup> remains equal to four: the rupture of an S–Cu bond is concomitant with the formation of a Cu–N bond *trans* to it (bond distances of 2.116 Å in water and 2.114 Å in acetonitrile), which results in an “open” cluster core structure. The longer Cu···S distance calculated for this structure (3.668 Å in water and 3.651 Å in acetonitrile) contrasts with the other two Cu–S bond lengths (average values of 2.519 Å in water and 2.518 Å in acetonitrile), which are similar to those found in [1]<sup>+</sup> and [2]<sup>+</sup>. This decoordination of sulfur from the Cu heteroatom raises the question about the heterobimetallic nature of the metal–metal bonds in cluster [4···H<sub>2</sub>O]<sup>+</sup>. The calculated Cu–W distances in this cluster are 3.070, 3.718 and 3.754 Å in water (with similar values obtained in acetonitrile), and hence one of the three Cu–W bonds originally present in the reactant remains. It is worth noting that the energy of the open [4···H<sub>2</sub>O]<sup>+</sup> cluster species is very close to that of the hydrated [1···H<sub>2</sub>O]<sup>+</sup> cluster, which means that it can provide accessible reaction pathways.

The two maxima represented in Figure 9 (**max1** and **max2**) correspond to the maxima linking the stationary points along the reaction path, namely [1···H<sub>2</sub>O]<sup>+</sup> plus CH<sub>3</sub>CN with [4···H<sub>2</sub>O]<sup>+</sup> (**max1**), and [4···H<sub>2</sub>O]<sup>+</sup> with [2]<sup>2+</sup> plus [Cl···H<sub>2</sub>O]<sup>-</sup> (**max2**). The geometries of **max1** and **max2** are depicted in Figure 10. The Cu–N distance along the re-

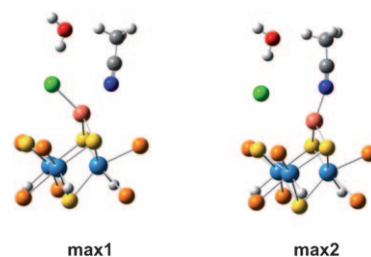
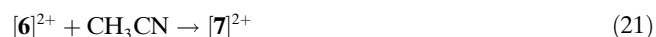
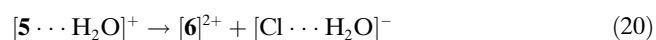


Figure 10. Gas-phase-optimised structures of **max1** and **max2**.

action coordinate (2.400 Å in **max1**) is higher than that corresponding to [4···H<sub>2</sub>O]<sup>+</sup> (2.115 Å), and one of the Cu–S distances increases from 3.463 Å in **max1** to 3.660 Å in [4···H<sub>2</sub>O]<sup>+</sup>. Alternatively, **max2** shows a decrease of the Cu–N and the Cu–S distances of 0.13 Å with respect to [4···H<sub>2</sub>O]<sup>+</sup>, thus recovering the cubane-type core cluster structure in the path to [2]<sup>2+</sup>. Rupture of the Cu–Cl bond occurs on going from [4···H<sub>2</sub>O]<sup>+</sup> to **max2**.

Because of the low energy barrier and almost thermoneutral character of the first step, intermediate [4···H<sub>2</sub>O]<sup>+</sup> can be considered to be formed in a rapid pre-equilibrium that is followed by rate-limiting chloride dissociation, which occurs with an activation barrier of 10.8 kcal mol<sup>-1</sup>. Although this activation barrier is in better agreement with the observed reaction rate values than that calculated for the dissociative mechanism, this mechanism is unable to explain the deceleration observed upon chloride addition, which

clearly indicates that chloride elimination takes place before the rate-determining step. For this reason, alternative reaction pathways involving the species  $[\text{W}_3\text{Cu}(\text{H}_2\text{O})(\text{Cl}\cdots\text{H}_2\text{O})\text{S}_4\text{H}_3(\text{dmpe})_3]^{2+}$  ( $[\mathbf{5}\cdots\text{H}_2\text{O}]^+$ ),  $[\text{W}_3\text{Cu}(\text{H}_2\text{O})\text{S}_4\text{H}_3(\text{dmpe})_3]^{2+}$  ( $[\mathbf{6}]^{2+}$ ) and  $[\text{W}_3\text{Cu}(\text{H}_2\text{O})(\text{CH}_3\text{CN})\text{S}_4\text{H}_3(\text{dmpe})_3]^{2+}$  ( $[\mathbf{7}]^{2+}$ ) were explored, and the mechanism depicted in Equations (19)–(22) were found to provide a more reasonable alternative.



The energy profile for this mechanism (Figure 11) indicates that intramolecular attack by a solvating water molecule of the  $[\mathbf{1}\cdots 2\text{H}_2\text{O}]^+$  species occurs with a low activation barrier of 4.2 kcal mol<sup>-1</sup> to give the “open” cluster core  $[\mathbf{5}\cdots\text{H}_2\text{O}]^+$ . Kinetically, this would be a less favourable step than the equivalent process involving acetonitrile represented in Figure 9. The activation barriers in both cases are, however, small and comparable, therefore both attacks are expected to be fast. Moreover,  $[\mathbf{5}\cdots\text{H}_2\text{O}]^+$  is around 4 kcal mol<sup>-1</sup> more stable than  $[\mathbf{4}\cdots\text{H}_2\text{O}]^+$  with respect to the reactants and so this species is expected to be formed in acetonitrile/water solutions. The next step in this mechanism involves release of the hydrated chloride, which occurs with an energy barrier of 2.4 kcal mol<sup>-1</sup> to yield the ion pair-like species  $[\mathbf{6}][\text{Cl}\cdots\text{H}_2\text{O}]^+$ , a stable intermediate (−9.5 kcal mol<sup>-1</sup>). A structural inspection of  $[\mathbf{6}][\text{Cl}\cdots\text{H}_2\text{O}]^+$  shows that dissociation of  $[\text{Cl}\cdots\text{H}_2\text{O}]^-$  from  $[\mathbf{5}\cdots\text{H}_2\text{O}]^+$  leads to recovery

of the cubane-like structure. There is a continuous energy increase from this point to the separated  $[\mathbf{6}]^{2+}$  and  $[\text{Cl}\cdots\text{H}_2\text{O}]^-$  species, as expected for a step involving separation of two species of different charge, hence the dissociation of chloride from  $[\mathbf{5}\cdots\text{H}_2\text{O}]^+$  can be described as occurring in two steps: decoordination of chloride from the copper atom coupled with sulfur recoordination, with the hydrated chloride still close by, and dissociation of the resulting ion-pair-like species. The acetonitrile molecule enters the copper coordination sphere in the next step, which results in decoordination of a sulfur atom and gives rise to the new open-cluster species  $[\mathbf{7}]^{2+}$ , which finally loses the water molecule attached to the Cu atom to yield the reaction products. The open-core species  $[\mathbf{5}\cdots\text{H}_2\text{O}]^+$  shows a large Cu–S distance (3.593 Å in acetonitrile, 3.590 Å in water), which indicates sulfur decoordination from the copper centre, while the water molecule has entered the coordination sphere of copper; the distance between Cu and the water oxygen is 2.089 Å in acetonitrile and 2.096 Å in water. The water ligand in  $[\mathbf{5}\cdots\text{H}_2\text{O}]^+$  is hydrogen-bonded to the uncoordinated sulfur atom (2.670 Å), which surely adds some contribution to the stabilisation energy. The second open-core cluster species appearing in Figure 11 corresponds to  $[\mathbf{7}]^{2+}$ . In this case, there is also a stabilizing hydrogen-bonding interaction between one hydrogen of the H<sub>2</sub>O ligand and the dissociated sulfur atom (2.481 Å). Figure 11 also includes the energies of three additional structures (**max3**, **max4** and **max5**) which correspond to the maxima along the scan calculations linking the stationary points  $[\mathbf{1}\cdots 2\text{H}_2\text{O}]^+$  with  $[\mathbf{5}\cdots\text{H}_2\text{O}]^+$  (**max3**),  $[\mathbf{5}\cdots\text{H}_2\text{O}]^+$  with the ion-pair-like structure (**max4**), and  $[\mathbf{7}]^{2+}$  with  $[\mathbf{2}]^{2+}$  (**max5**). The geometries of **max3**, **max4** and **max5** are in agreement with each ligand substitution step, as shown in Figure 12.

This mechanism can account for the experimental results in a better way than those discussed above because the dissociation of Cl<sup>-</sup> from the copper centre occurs in an intermediate step before the rate-determining one. Furthermore, the smoothness of the energy profile, the accessibility of the energy barriers under normal reaction conditions, and the fact that the overall process is not too energy-demanding ensure that this mechanism is possible under the experimental reaction conditions. The highest energy point in Figure 11 corresponds to **max5**, that is, to the barrier for dissociation of water from  $[\mathbf{7}]^{2+}$  in a step that follows chloride dissociation. Thus, the processes in Equations (19)–(22) could occur as rapid pre-equilibria

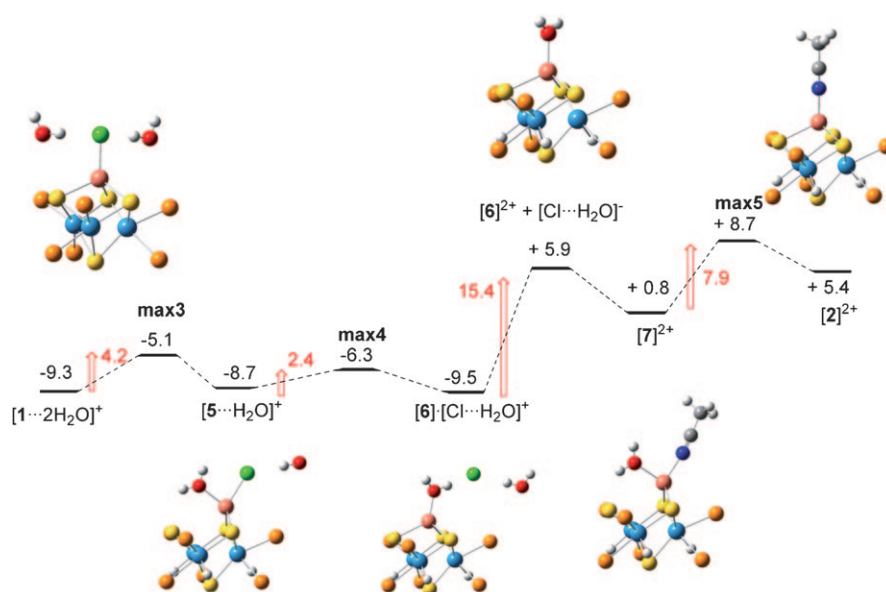


Figure 11. Energy profile [kcal mol<sup>-1</sup>] in CH<sub>3</sub>CN/H<sub>2</sub>O (1:1) for the mechanism represented in Equations (19)–(22).

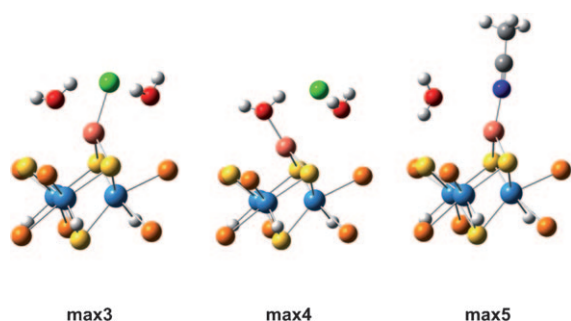


Figure 12. Schematic representation of **max3**, **max4** and **max5**.

leading to small amounts of  $[5]^{2+}$ ,  $[6]^{2+}$  and  $[7]^{2+}$ ; the rate-determining step would be the process in Equation (22). In any case, DFT calculations clearly reveal the possibility of opening-up of the cluster core by water and acetonitrile and that the resulting products can provide reaction pathways for substitution of coordinated chloride more efficiently than a simple dissociative mechanism in which the integrity of the cluster is retained.

**The quest for experimental evidence for the formation of open-core cluster structures:**

In addition to the substitution of the coordinated chloride discussed above, the open-core cluster species described in previous sections also represent a rational starting point for reaction pathways leading to the experimentally observed fragmentation of  $[2]^{2+}$  to afford the trinuclear cluster and  $\text{Cu}(\text{NCCH}_3)$  fragments. Although the existence of reaction intermediates with open-core cluster structures has already been postulated,<sup>[20]</sup> to the best of our knowledge there is no direct experimental evidence of their presence or of the factors that favour their formation. This work shows that operation of the mechanism in Equations (19)–(22) could lead to the formation of small amounts of the open-core species  $[5 \cdots \text{H}_2\text{O}]^{2+}$  and  $[7]^{2+}$ . Moreover, according to the DFT results, significant amounts of  $[4 \cdots \text{H}_2\text{O}]^+$  could also be formed even in acetonitrile solution, where traces of water promote the substitution process and lead to small amounts of  $[2]^{2+}$ . For these reasons, the possibility of detecting some of these species by NMR spectroscopic and ESI-MS techniques was explored both in acetonitrile and in solutions containing added water.

Unfortunately, NMR experiments were of no help at this point. As the opening of the cluster core causes the molecular symmetry to decrease, the formation of open-core cluster species would be expected to

lead to more complex  $^{31}\text{P}$  NMR spectra, which is not observed experimentally. Nevertheless, this finding does not rule out the possibility that these species are formed. It is likely that open-core clusters are formed as minor species in equilibrium with the unperturbed starting cluster, which means that their concentration could be below the detection limit of the technique. Moreover, it should also be considered that different Cu–S bonds are broken each time, thus causing the averaging of the NMR signals and the appearance of simple two-signal spectra, as found experimentally.

The ESI mass spectra of acetonitrile solutions of  $[1]\text{PF}_6$  obtained under mild conditions (at a low cone voltage of 5 V) show the expected pseudo-molecular ion  $[1]^+$  ( $m/z$  1232.9) as the base peak. The ESI mass spectra recorded after the sequential addition of aliquots of water to acetonitrile solutions of  $[1]\text{PF}_6$  show that the relative intensity of the signal of  $[1]^+$  decreases and the intensity of the signal due to  $[2]^{2+}$  ( $m/z$  618.5) increases. The ESI mass spectra also reveal an identical chemical speciation, irrespective of the acetonitrile/water ratio used as solvent, with the relative intensity of the species detected being the most significant difference. Remarkably, the temporal evolution of the species detected remains largely unchanged (typically 20 minutes), thus suggesting that equilibration is reached rapidly after increasing the water content. Figure 13 illustrates the ESI mass spectrum of acetonitrile/water (3:1) solutions of compound  $[1]\text{PF}_6$ .

Besides the presence of unreacted  $[1]^+$  ( $m/z$  1232.9), the ESI mass spectrum shows a minor signal centred at  $m/z$  1250.9 which, on the basis of its  $m/z$  value and the isotopic distribution, formally corresponds to the addition of one water molecule to the  $[1]^+$  cation. Interestingly, this cation is invoked as a crucial species in our proposed mechanistic picture in the form of two plausible isomers, namely  $[1 \cdots \text{H}_2\text{O}]^+$  or  $[5]^+$  (see Figures 9 and 11, respectively). The ESI mass spectrum also shows additional signals centred at

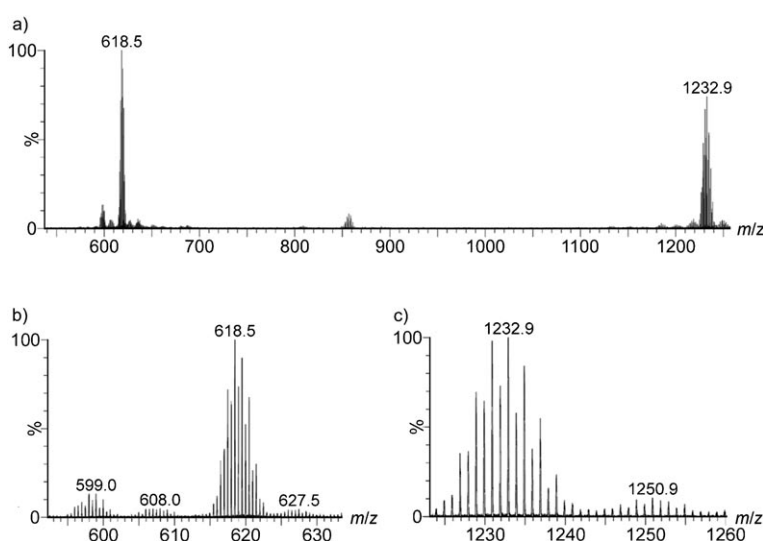


Figure 13. a) ESI mass spectrum of compound  $[1]\text{PF}_6$  in  $\text{CH}_3\text{CN}/\text{H}_2\text{O}$  (3:1). b) Expansion of the region  $m/z$  590–630 and c) expansion of the region  $m/z$  1220–1260.

$m/z$  598.0, 607.0 and 627.5 assignable to the dications [3]<sup>2+</sup>, [6]<sup>2+</sup> and [7]<sup>2+</sup>, respectively. The experimental detection of dication [3]<sup>2+</sup> suggests the operation of a simple dissociative mechanism to account for the [1]<sup>+</sup> to [2]<sup>2+</sup> transformation (see Figure 8); however, the formation of cation [3]<sup>2+</sup> as a consequence of gas-phase dissociation of dications [6]<sup>2+</sup> and [7]<sup>2+</sup> during the ESI process cannot be definitively ruled out. Indeed, ESI-MS/MS of the solvent-coordinated [6]<sup>2+</sup> and [7]<sup>2+</sup> dications affords [3]<sup>2+</sup> as the only product ion at low collision energies, thus indicating that the observation of [3]<sup>2+</sup> likely results from the gas-phase dissociation of [6]<sup>2+</sup> and [7]<sup>2+</sup>. When the amount of water in the CH<sub>3</sub>CN/H<sub>2</sub>O mixtures is increased, the ESI mass spectra reveal the exclusive presence of the [2]<sup>2+</sup> dication as the base peak, thus confirming the progressive conversion of [1]<sup>+</sup> into [2]<sup>2+</sup>. The ESI mass spectrometric characterisation of dications [6]<sup>2+</sup> and [7]<sup>2+</sup> and species [5]<sup>+</sup> (on the basis of either  $m/z$  values or isotopic pattern simulations), and the absence of the signal corresponding to [4]<sup>+</sup> ( $m/z$  1273.9), strongly supports the mechanism in Equations (19)–(22). These ESI mass spectrometric experiments provide firm evidence regarding the formation of minor amounts of open-core cluster species, thus supporting the operation of the mechanism proposed above on the basis of DFT calculations.

## Conclusion

The heterodimetallic W<sub>3</sub>CuS<sub>4</sub> hydride cubane-type complexes [1]<sup>+</sup> and [2]<sup>2+</sup> have been synthesised for the first time by incorporation of CuCl or Cu(NCCH<sub>3</sub>)<sup>+</sup> into [W<sub>3</sub>S<sub>4</sub>H<sub>3</sub>(dmpe)<sub>3</sub>]<sup>+</sup>, respectively. Insertion of the heterometal causes a decrease of the acidity of the W-H sites. The crystallographic parameters of cluster [1]<sup>+</sup> show that there are no significant changes in W–W bond lengths upon copper coordination, as observed in the analogous W<sub>3</sub>CuS<sub>4</sub> bromide cluster.<sup>[21]</sup> However, an expansion of the S<sub>4</sub> tetrahedron similar to that previously observed in a related Pd complex occurs.<sup>[29]</sup> Elongation of the heterometal–sulfur bond has also been described by Holm and co-workers in Fe<sub>3</sub>M'S<sub>4</sub> (M' = Ni, Pd, Pt) clusters, where a distorted *cubanoïd* structure of the cluster-core unit reproduces the crystallographic structures of carbon monoxide dehydrogenases.<sup>[45]</sup> The most interesting feature in the chemical behaviour of these compounds, however, is an unexpected conversion of [1]<sup>+</sup> into [2]<sup>2+</sup> that involves substitution of chloride by acetonitrile at the copper centre. This process is favoured by the presence of water both from a thermodynamic and kinetic point of view; that is, added water displaces the reaction towards the acetonitrile complex and the reaction rate increases with the amount of water added. Computational studies have led to a rationalisation of these results and a mechanistic proposal in which the opening of the cluster core plays a fundamental role. These open-core species can be formed by attack of acetonitrile or water on the cluster, and their formation involves the breaking of one of the Cu–S bonds; that is, the coordination mode of the heterometal-

lic Cu centre to the trinuclear W<sub>3</sub>S<sub>4</sub> fragment changes during the reaction to accommodate the entering ligand. The mechanism proposed for this reaction resembles in some way the well-established ring slippage in cyclopentadienido–metal complexes,<sup>[46–52]</sup> where the hapticity of the Cp ligand is reduced to accommodate an entering ligand. Similar processes have also been proposed to be relevant in the chemistry of metallatricarbodecaboranyl complexes,<sup>[53–55]</sup> and the opening of carbonyl clusters has also been reported to be an available reaction pathway for ligand addition or substitution.<sup>[56,57]</sup>

The possibility of opening the cluster structure proposed in this paper clearly adds new perspectives to the classical description of the reactivity pattern of M<sub>3</sub>M'Q<sub>4</sub> (M = Mo, W; Q = S, Se) cubane-type clusters, whereby the presence of metal–metal bonds in the cluster simply tunes the reaction rates with only limited, if any, communication between the metals.<sup>[29]</sup> The opening of the cluster core also allows for the transient appearance of an additional coordination site at the M' site which could explain the reported reactivity and catalytic activities centred on the heterometal in Mo<sub>3</sub>M'S<sub>4</sub> derivatives when M' is Ni, Pd, Ru. The oxidation state of the heterometal in these clusters does not always present well-defined values, thereby adding new interest to their potential activity in catalysis. For the particular case of Mo<sub>3</sub>CuS<sub>4</sub> clusters with diphosphanes, the lability of the sulfur ligands can explain the activity and stability of these stable Cu<sup>I</sup> cluster compounds in the inter- and intramolecular cyclopropanation of olefins. Despite the significant differences between these compounds and the more biologically relevant Fe/S cluster complexes, the occurrence of similar processes in the latter is a possibility to be considered.

## Experimental Section

[W<sub>3</sub>S<sub>4</sub>H<sub>3</sub>(dmpe)<sub>3</sub>]PF<sub>6</sub> was prepared according to literature methods.<sup>[58]</sup> CuCl was obtained from commercial sources and [Cu(CH<sub>3</sub>CN)<sub>4</sub>]PF<sub>6</sub> was synthesised from commercial Cu<sub>2</sub>O and HPF<sub>6</sub> in acetonitrile.<sup>[59]</sup> Solvents for synthesis and electrochemical measurements were dried and degassed by standard methods before use.

**Physical measurements:** Elemental analyses were performed with an EA 1108 CHNS microanalyzer at the Universidad de La Laguna. <sup>31</sup>P{<sup>1</sup>H} NMR spectra were recorded with either a Varian Mercury 300 or a Varian Unity 400 MHz spectrometer and were referenced to external 85% H<sub>3</sub>PO<sub>4</sub>. <sup>1</sup>H and <sup>13</sup>C{<sup>1</sup>H} spectra were recorded with a Varian Inova 500 MHz spectrometer; the chemical shifts are reported in ppm from tetramethylsilane with the solvent resonance taken as the internal standard. IR spectra were recorded with a Perkin–Elmer System 2000 FT-IR using KBr pellets. Electronic absorption spectra were obtained with a Perkin–Elmer Lambda-19 spectrophotometer for samples in dichloromethane. A hybrid QTOF I (quadrupole-hexapole-TOF) mass spectrometer with an orthogonal Z-spray-electrospray interface (Waters, Manchester, UK) was used to measure the mass spectra. The drying and nebulising gas was nitrogen at a flow of 800 and 30 L/h, respectively. The temperature of the source block was set to 100°C and the desolvation temperature to 120°C. A capillary voltage of 3.5 kV was used in the positive scan mode, and the cone voltage was set to 5 V unless otherwise stated. Increasing amounts of water were added to acetonitrile solutions of compound [1]PF<sub>6</sub> and the resulting mixture was infused with a syringe pump connected directly to the ESI source at a flow rate of 10 μL/min. Different sample concen-

trations were employed (typically between  $5 \times 10^{-3}$  and  $1 \times 10^{-5}$  M) and the results were comparable. The observed isotopic pattern of each intermediate perfectly matched the theoretical isotope pattern calculated from their elemental composition using the MassLynx 4.0 program. ESI MS/MS spectra were obtained at various collision energies (typically 0–15 eV) by selecting the precursor ion of interest with the first quadrupole (Q1) with an isolation width of approximately 1 Da and analysing the product ions with the time of flight analyzer (TOF). Argon was used as collision gas and the pressure in the collision cell was maintained at  $4 \times 10^{-5}$  mbar.

#### Synthesis

$[W_3CuClS_4H_3(dmpc)_3]PF_6$  (**[1]** $(PF_6)_6$ ): CuCl (0.08 g, 0.09 mmol) was added to a solution of  $[W_3S_4H_3(dmpc)_3]PF_6$  (0.09 g, 0.07 mmol) in  $CH_2Cl_2$  (40 mL) under nitrogen at room temperature, and a colour change from pink to red was observed immediately. After stirring for 2 h, the reaction mixture was filtered and the resulting solution was taken to dryness to afford a red microcrystalline product which was subsequently characterised as **[1]** $(PF_6)_6$  (yield: 0.09 g, 93%). Elemental analysis calcd. for  $C_{18}H_{51}ClCuF_6P_7S_4W_3$  (1377.2): C 15.70, H 3.73, S 9.31; found: C 15.75, H 3.72, S 9.25.  $^1H$  NMR ( $CD_3CN$ ):  $\delta = 0.17$  (dd,  $^2J_{PH} = 47.5$ ,  $^2J_{P,H} = 28.5$  Hz, 3H; hydride), 0.76 (d,  $^2J_{PH} = 9.0$  Hz, 9H;  $CH_3$ ), 1.89 (m, 3H;  $CH_2$ ), 2.05 (d,  $^2J_{PH} = 10.2$  Hz, 9H;  $CH_3$ ), 2.14 (m, 3H;  $CH_2$ ), 2.24 (d,  $^2J_{PH} = 9.5$  Hz, 9H;  $CH_3$ ), 2.29 (m, 3H;  $CH_2$ ), 2.33 (d,  $^2J_{PH} = 9.3$  Hz, 9H;  $CH_2$ ), 2.88 (m, 3H;  $CH_2$ );  $^{13}C\{^1H\}$  NMR ( $CD_3CN$ ):  $\delta = 14.57$  (d,  $^1J_{CP} = 22.4$  Hz;  $CH_3$ ), 21.17 (d,  $^1J_{CP} = 19.6$  Hz;  $CH_3$ ), 21.52 (d,  $^1J_{CP} = 12.0$  Hz;  $CH_3$ ), 21.99 (d,  $^1J_{CP} = 33.3$  Hz;  $CH_3$ ), 28.78 (dd,  $^1J_{CP} = 30.0$  Hz,  $^2J_{CP} = 10.4$  Hz;  $CH_2$ ), 29.35 (dd,  $^1J_{CP} = 36.0$  Hz,  $^2J_{CP} = 10.9$  Hz;  $CH_2$ );  $^{31}P\{^1H\}$  NMR ( $CD_2Cl_2$ ):  $\delta = -143.85$  (sept,  $^1J_{PF} = 704.0$  Hz),  $-8.90$  (s,  $^1J_{PW} = 125.8$  Hz), 0.69 (s,  $^1J_{PW} = 175.4$  Hz); IR (KBr):  $\tilde{\nu} = 1769$  (m, W–H), 1093 (s), 937 (i), 841 (i, P–F), 748 (m), 653 (m), 558 (i, P–F), 406 (w), 342 (d); UV/Vis ( $CH_2Cl_2$ ):  $\lambda = 517, 408, 302$  (sh), 264, 232 nm; ESI-MS ( $CH_2Cl_2$ , 85 V):  $m/z$ : 1232.9 [ $M^+$ ], 982.9 [ $M^+ - CuCl - dmpc$ ].

$[W_3Cu(CH_3CN)S_4H_3(dmpc)_3](PF_6)_2$  (**[2]** $(PF_6)_2$ ):  $[Cu(CH_3CN)_4]PF_6$  (0.08 g, 0.09 mmol) was added to a solution of  $[W_3S_4H_3(dmpc)_3]PF_6$  (0.10 g, 0.08 mmol) in  $CH_2Cl_2$  (40 mL) under nitrogen at room temperature, and a colour change from pink to red was observed immediately. After 2 h of stirring, the reaction mixture was filtered and the resulting solution was taken to dryness to afford a red microcrystalline product, which was subsequently characterised as **[2]** $(PF_6)_2$ . This product decomposes after 3 h in solution. (yield 0.10 g, 83%). Elemental analysis calcd. for  $C_{20}H_{54}CuF_{12}NP_8S_4W_3$  (1527.8): C 15.72, H 3.56, N 0.92, S 8.39; found: C 15.71, H 3.67, N 0.88, S 8.34.  $^1H$  NMR ( $CD_3CN$ ):  $\delta = 0.11$  (dd,  $^2J_{PH} = 48.7$ ,  $^2J_{P,H} = 29.3$  Hz, 3H; hydride), 0.71 (d,  $^2J_{PH} = 9.5$  Hz, 9H;  $CH_3$ ), 1.84 (m, 3H;  $CH_2$ ), 1.99 (d,  $^2J_{PH} = 10.4$  Hz, 9H;  $CH_3$ ), 2.10 (m, 3H;  $CH_2$ ), 2.18 (d,  $^2J_{PH} = 9.68$  Hz, 9H;  $CH_3$ ), 2.25 (3H,  $CH_2$ ; m), 2.28 (d,  $^2J_{PH} = 9.35$  Hz, 9H;  $CH_3$ ), 2.81 (m, 3H;  $CH_2$ );  $^{13}C\{^1H\}$  NMR ( $CD_3CN$ ):  $\delta = 18.81$  (d,  $^1J_{CP} = 22.9$  Hz;  $CH_3$ ), 25.41 (d,  $^1J_{CP} = 39.4$  Hz,  $CH_3$ ), 25.36 (d,  $^1J_{CP} = 30.7$  Hz;  $CH_3$ ), 26.24 (d,  $^1J_{CP} = 34.8$  Hz;  $CH_3$ ), 33.02 (dd,  $^1J_{CP} = 30.7$  Hz,  $^2J_{CP} = 9.6$  Hz;  $CH_2$ ), 33.60 (dd,  $^1J_{CP} = 35.3$  Hz,  $^2J_{CP} = 10.5$  Hz;  $CH_2$ );  $^{31}P\{^1H\}$  NMR ( $CD_3CN$ ):  $\delta = -143.80$  (sept,  $^1J_{PF} = 704.0$  Hz),  $-4.00$  (s,  $^1J_{PW} = 118.2$  Hz), 5.90 (s,  $^1J_{PW} = 176.0$  Hz); IR (KBr):  $\tilde{\nu} = 2245$  (s, CN), 1769 (m, W–H), 1681 (i, CN), 1644 (i, CN), 1419 (i), 1318 (i), 1288 (m), 1140 (m), 1085 (m), 1054 (m), 938 (i), 839 (i, P–F), 558 (i, P–F), 476 (w), 338 (d); UV/Vis ( $CH_3CN$ ):  $\lambda = 508, 360, 303$  nm; ESI-MS ( $CH_2Cl_2$ , 25 V):  $m/z$ : 618.5 [ $M^{2+}$ ], 598.0 [ $M^{2+} - CH_3CN$ ].

**Kinetic experiments:** The kinetic experiments were carried out with an Applied Photophysics SX17 MV stopped-flow spectrometer equipped with a PDA1 photodiode array (PDA) detector. All experiments were carried out at 25.0 °C by mixing an acetonitrile solution of **[1]** $(PF_6)_6$  with an  $H_2O$ ,  $CH_3CN$  or  $CH_3CN/H_2O$  solution containing the amount of  $Et_4NBF_4$  required to achieve a constant ionic strength of 0.1 M in the solution arriving in the stopped-flow cell. Some experiments were carried out in presence of  $Et_4NCl$  by adding the required amount of this salt together with the  $Et_4NBF_4$  required to achieve the desired ionic strength. The solutions of the complex were prepared at a concentrations of around  $1.0 \times 10^{-3}$  M, and preliminary experiments were carried out for each reaction at two or three different complex concentrations to confirm the first-order dependence of the observed rate constants with respect to the complex. The re-

action kinetics were monitored by recording the spectral changes with time using the PDA detector, and the data were analysed with the SPEC-FIT program using the appropriate kinetic model.<sup>[60]</sup> Reported values for the rate constant correspond to the mean value of at least five determinations, the standard deviation being lower than 5% in all cases.

**X-ray diffraction studies:** Crystals of compound **[1]** $(PF_6)_6$  suitable for X-ray studies were grown by slow diffusion of diethyl ether into a sample solution in  $CH_2Cl_2$ . The red crystals obtained are air stable and were mounted on the tip of a glass fibre with the use of epoxy cement. X-ray diffraction experiments were carried out with a Bruker SMART CCD diffractometer using  $MoK_{\alpha}$  radiation ( $\lambda = 0.71073$  Å) at room temperature. The data were collected with a frame width of  $0.3^\circ$  in  $\omega$  and a counting time of 20 s per frame. The diffraction frames were integrated using the SAINT package and corrected for absorption with SADABS.<sup>[61,62]</sup> The structures were solved by direct methods and refined by the full-matrix method based on  $F^2$  using the SHELXTL software package.<sup>[63]</sup> The structure of **[1]** $(PF_6)_6$  was successfully solved in the hexagonal  $P6_3$  space group. This structure was solved taking into account a racemic twinning yielding a flack parameter of 0.518(15). All cluster atoms were refined anisotropically, whereas the positions of the hydrogen atoms from the diphosphane backbone were generated geometrically, assigned isotropic thermal parameters and allowed to ride on their respective parent carbon atoms. The C(2)–C(3) bond distance for the carbon atoms in the ethylene bridge of the diphosphane was constrained at a fixed value. One independent  $PF_6^-$  anion was found in a special position; only the phosphorus atom was refined anisotropically. One molecule of dichloromethane was encountered in the latest Fourier density map and refined isotropically as a rigid group. Crystal data for **[1]** $(PF_6)_6$ :  $C_{18}H_{51}ClCuF_6P_7S_4W_3$ ,  $M = 1462.08$ , hexagonal, space group  $P6_3$ ,  $a = 12.639(2)$ ,  $b = 12.639(2)$ ,  $c = 15.748(4)$  Å,  $V = 2178.7(8)$  Å<sup>3</sup>,  $T = 293$  K,  $Z = 2$ ,  $\rho_{calcd} = 2.229$  g cm<sup>−3</sup>,  $\mu(MoK_{\alpha}) = 9.049$  mm<sup>−1</sup>. Reflections collected/unique = 15 133/3002 ( $R_{int} = 0.0456$ ). Final refinement converged with  $R_1 = 0.0299$  for 2416 reflections with  $F_0 = 4\sigma(F_0)$  and  $wR_2 = 0.0714$  for all reflections,  $GoF = 1.039$ , max./min. residual electron density 0.953 and  $-1.255$  e Å<sup>−3</sup>.

**Theoretical calculations:** All calculations were performed with the Gaussian03 package<sup>[64]</sup> at the B3LYP level.<sup>[65,66]</sup> All atoms were represented by the relativistic core potential (LanL2) from Los Alamos with an associated double- $z$  pseudo-orbital basis set.<sup>[64,67]</sup> Phosphorus atoms were augmented by a  $p$  ( $\alpha = 0.0298$ ) and  $d$  ( $\alpha = 0.364$ ) polarisation and diffuse functions.<sup>[68]</sup> The geometry optimisations for each intermediate were performed without any symmetry constraint followed by analytical frequency calculations to confirm that a minimum had been reached. The potential energy surface scan calculations were done by increasing the selected reaction coordinate with a 0.10–0.20 Å step size. The energies of all systems studied at the B3LYP level in the gas phase were recomputed with single point calculations, in the case of the maxima of the scan, and reoptimised, for each intermediate, by inclusion of solvent effects for acetonitrile ( $\epsilon = 36.64$ ) and water ( $\epsilon = 78.39$ ) according to the Polarizable Continuum Model (PCM) scheme, as implemented in Gaussian. The united atom topological model with UAHF radii was used.<sup>[69,70]</sup> Energies in  $CH_3CN/H_2O$  (1:1) mixtures were estimated as the average of computed energies in acetonitrile and water as solvent. We used electronic PCM energies ( $E$ ) and not Gibbs energies ( $G$ ) to characterise the reaction paths due to the difficulties encountered when calculating the entropy in condensed phases. Several alternatives have been suggested in the literature, some of which completely neglect translational entropy, which is the greatest contribution to the total entropy term.<sup>[71–75]</sup>

## Acknowledgments

This work was supported by the Spanish Ministerio de Educación y Ciencia (projects CTQ2006-15447-C02-01 and CTQ2006-14909-C02-01), the Ministerio de Ciencia e Innovación (project CTQ2008-02670/BQU), and the Fundació Bancaixa-Universitat Jaume I (grants P1.1B2007-12 and P1.1B2005-15). M.F. thanks the Fundació UJI-Bancaixa for a visiting researcher grant. A.G.A. acknowledges a predoctoral grant from the Span-

ish Ministerio de Ciencia y Tecnología. The authors also thank the Servei Central D'Instrumentació Científica (SCIC) and Servei d'Informàtica de the Universitat Jaume I and the Servicios Centrales de Ciencia y Tecnología of the Universidad de Cádiz for providing us with the mass spectrometry, NMR, X-ray and computing facilities.

- [1] I. Dance, K. Fisher, *Prog. Inorg. Chem.* **1994**, *41*, 637.
- [2] U. Riaz, O. J. Curnow, M. D. Curtis, *J. Am. Chem. Soc.* **1994**, *116*, 4357.
- [3] D. M. Curtis in *Transition metal sulfur chemistry: biological and industrial significance*, Vol. 653 (Eds.: E. I. Stiefel, K. Matsumoto), ACS, Washington, **1996**, pp. 154.
- [4] H. Beinert, R. H. Holm, E. Munck, *Science* **1997**, *277*, 653.
- [5] I. Takei, K. Kobayashi, K. Dohki, S. Nagao, Y. Mizobe, M. Hidai, *Chem. Lett.* **2007**, *36*, 546.
- [6] I. Takei, K. Suzuki, Y. Enta, K. Dohki, T. Suzuki, Y. Mizobe, M. Hidai, *Organometallics* **2003**, *22*, 1790.
- [7] T. Murata, Y. Mizobe, H. Gao, Y. Ishii, T. Wakabayashi, F. Nakano, T. Tanase, S. Yano, M. Hidai, I. Echizen, H. Nanikawa, S. Motomura, *J. Am. Chem. Soc.* **1994**, *116*, 3389.
- [8] R. Hernandez-Molina, A. G. Sykes, *Coord. Chem. Rev.* **1999**, *187*, 291.
- [9] D. M. Saysell, C. D. Borman, C. H. Kwak, A. G. Sykes, *Inorg. Chem.* **1996**, *35*, 173.
- [10] M. N. Sokolov, E. V. Chubarova, K. A. Kovalenko, I. V. Mironov, A. V. Virovets, E. V. Peresyphkina, V. P. Fedin, *Russ. Chem. Bull.* **2005**, *54*, 615.
- [11] R. Hernández-Molina, I. Kalinina, M. Sokolov, M. Clausen, J. G. Platas, C. Vicent, R. Llusar, *Dalton Trans.* **2007**, 550.
- [12] R. Hernández-Molina, M. N. Sokolov, M. Clausen, W. Clegg, *Inorg. Chem.* **2006**, *45*, 10567.
- [13] A. G. Algarra, M. G. Basallote, M. J. Fernandez-Trujillo, R. Hernandez-Molina, V. S. Safont, *Chem. Commun.* **2007**, 3071.
- [14] I. Takei, Y. Enta, Y. Wakebe, T. Suzuki, M. Hidai, *Chem. Lett.* **2006**, *35*, 590.
- [15] I. Takei, Y. Wakebe, K. Suzuki, Y. Enta, T. Suzuki, Y. Mizobe, M. Hidai, *Organometallics* **2003**, *22*, 4639.
- [16] M. Taniguchi, D. Imamura, H. Ishige, Y. Ishii, T. Murata, M. Hidai, T. Tatsumi, *J. Catal.* **1999**, *187*, 139.
- [17] M. Feliz, R. Llusar, S. Uriel, C. Vicent, M. Brorson, K. Herbst, *Polyhedron* **2005**, *24*, 1212.
- [18] L. Takei, K. Dohki, K. Kobayashi, T. Suzuki, M. Hidai, *Inorg. Chem.* **2005**, *44*, 3768.
- [19] M. Feliz, E. Guillamon, R. Llusar, C. Vicent, S. E. Stiriba, J. Perez-Prieto, M. Barberis, *Chem. Eur. J.* **2006**, *12*, 1486.
- [20] E. Guillamon, R. Llusar, J. Perez-Prieto, S. E. Stiriba, *J. Organomet. Chem.* **2008**, *693*, 1723.
- [21] M. Feliz, J. M. Garriga, R. Llusar, S. Uriel, M. G. Humphrey, N. T. Lucas, M. Samoc, B. Luther-Davies, *Inorg. Chem.* **2001**, *40*, 6132.
- [22] H. Zhan, Y. Zheng, X. Wu, J. Lu, *Inorg. Chim. Acta* **1989**, *156*, 277.
- [23] X. Wu, S. Lu, L. Zu, Q. Wu, J. Lu, *Inorg. Chim. Acta* **1987**, *133*, 39.
- [24] Y. Zheng, H. Zhan, X. Wu, J. Lu, *Transition Met. Chem.* **1989**, *14*, 161.
- [25] K. Herbst, M. Monari, M. Brorson, *Inorg. Chim. Acta* **2004**, *357*, 895.
- [26] S. F. Fu, H. B. Chen, J. Q. Huang, Q. J. Wu, Q. L. Sun, J. Li, J. X. Lu, *Inorg. Chim. Acta* **1995**, *232*, 43.
- [27] H. Diller, H. Keck, W. Kuchen, D. Mootz, R. Wiskemann, *Zeitsch. Naturforsch. B* **1993**, *48*, 291.
- [28] H. Akashi, T. Shibahara, *Inorg. Chim. Acta* **2000**, *300–302*, 572.
- [29] A. G. Algarra, M. G. Basallote, M. Feliz, M. J. Fernández-Trujillo, E. Guillamón, R. Llusar, C. Vicent, *Inorg. Chem.* **2006**, *45*, 5576.
- [30] A. G. Algarra, M. G. Basallote, M. Feliz, M. J. Fernandez-Trujillo, R. Llusar, V. S. Safont, *Chem. Eur. J.* **2006**, *12*, 1413.
- [31] M. G. Basallote, M. Feliz, M. J. Fernandez-Trujillo, R. Llusar, V. S. Safont, S. Uriel, *Chem. Eur. J.* **2004**, *10*, 1463.
- [32] M. G. Basallote, F. Estevan, M. Feliz, M. J. Fernandez-Trujillo, D. A. Hoyos, R. Llusar, S. Uriel, C. Vicent, *Dalton Trans.* **2004**, 530.
- [33] N. A. Stephenson, A. T. Bell, *Inorg. Chem.* **2007**, *46*, 2278.
- [34] N. A. Stephenson, A. T. Bell, *Inorg. Chem.* **2006**, *45*, 2758.
- [35] N. A. Stephenson, A. T. Bell, *J. Am. Chem. Soc.* **2005**, *127*, 8635.
- [36] R. Llusar, S. Uriel, *Eur. J. Inorg. Chem.* **2003**, 1271.
- [37] T. Shibahara, *Coord. Chem. Rev.* **1993**, *123*, 73.
- [38] R. Hernández-Molina, A. G. Sykes, *J. Chem. Soc. Dalton Trans.* **1999**, 3137.
- [39] Y. Marcus, *Chem. Rev.* **2007**, *107*, 3880.
- [40] E. A. Goma, *Thermochim. Acta* **1989**, *152*, 371.
- [41] R. G. Wilkins, *Kinetics and Mechanisms of Reactions of Transition Metal Complexes*, VCH, Weinheim, **1991**.
- [42] L. G. Gagliardi, C. B. Castells, C. Rafols, M. Roses, E. Bosch, *J. Chem. Eng. Data* **2007**, *52*, 1103.
- [43] R. Ayala, J. M. Martinez, R. R. Pappalardo, E. S. Marcos, *J. Phys. Chem. A* **2000**, *104*, 2799.
- [44] G. Saielli, G. Scorrano, A. Bagno, A. Wakisaka, *Chemphyschem* **2005**, *6*, 1307.
- [45] R. Panda, C. P. Berlinguette, Y. Zhang, R. H. Holm, *J. Am. Chem. Soc.* **2005**, *127*, 11092.
- [46] T. Privalov, J. S. M. Samec, J. E. Backvall, *Organometallics* **2007**, *26*, 2840.
- [47] T. Mizuta, Y. Imamura, K. Miyoshi, *J. Am. Chem. Soc.* **2003**, *125*, 2068.
- [48] H. J. Fan, M. B. Hall, *Organometallics* **2001**, *20*, 5724.
- [49] W. Simanko, W. Tesch, V. N. Sapunov, K. Mereiter, R. Schmid, K. Kirchner, J. Coddington, S. Wherland, *Organometallics* **1998**, *17*, 5674.
- [50] W. Simanko, V. N. Sapunov, R. Schmid, K. Kirchner, S. Wherland, *Organometallics* **1998**, *17*, 2391.
- [51] F. Basolo, *New J. Chem.* **1994**, *18*, 19.
- [52] J. M. O'Connor, C. P. Casey, *Chem. Rev.* **1987**, *64*, 307.
- [53] B. M. Ramachandran, S. M. Trupia, W. E. Geiger, P. J. Carroll, L. G. Sneddon, *Organometallics* **2002**, *21*, 5078.
- [54] B. M. Ramachandran, P. J. Carroll, L. G. Sneddon, *J. Am. Chem. Soc.* **2000**, *122*, 11033.
- [55] R. Butterick, B. M. Ramachandran, P. J. Carroll, L. G. Sneddon, *J. Am. Chem. Soc.* **2006**, *128*, 8626.
- [56] R. D. Adams, Y. Chi, D. D. Desmarquette, D. Lentz, R. Marschall, A. Scherrmann, *J. Am. Chem. Soc.* **1992**, *114*, 10822.
- [57] R. D. Adams, B. Captain, L. Zhu, *J. Am. Chem. Soc.* **2007**, *129*, 2454.
- [58] F. A. Cotton, R. Llusar, C. T. Eagle, *J. Am. Chem. Soc.* **1989**, *111*, 4332.
- [59] G. J. Kubas, *Inorg. Synth.* **1979**, *19*, 90.
- [60] R. A. Binstead, B. Jung, A. D. Zuberbühler in *SPECFIT-32*, Spectrum Software Associates, Chappel Hill, **2000**.
- [61] B.A.X.-R. Systems in *SAINT 6.2*, Bruker Analytical X-ray Systems, Madison, **2001**.
- [62] G. M. Sheldrich in *SADABS empirical absorption program*, University of Göttingen, **1996**.
- [63] G. M. Sheldrich in *SHELXTL*, Bruker Analytical X-ray Systems, Madison, **1997**.
- [64] Gaussian 03, Revision E.01, M. J. Frisch, G. W. Trucks, H. B. Schlegel, G. E. Scuseria, M. A. Robb, J. R. Cheeseman, V. G. Zakrzewski, J. A. Montgomery, Jr., R. E. Stratmann, J. C. Burant, S. Dapprich, J. M. Millam, A. D. Daniels, K. N. Kudin, M. C. Strain, O. Farkas, J. Tomasi, V. Barone, M. Cossi, R. Cammi, B. Mennucci, C. Pomelli, C. Adamo, S. Clifford, J. Ochterski, G. A. Petersson, P. Y. Ayala, Q. Cui, K. Morokuma, P. Salvador, J. J. Dannenberg, D. K. Malick, A. D. Rabuck, K. Raghavachari, J. B. Foresman, J. Cioslowski, J. V. Ortiz, A. G. Baboul, B. B. Stefanov, G. Liu, A. Liashenko, P. Piskorz, I. Komaromi, R. Gomperts, R. L. Martin, D. J. Fox, T. Keith, M. A. Al-Laham, C. Y. Peng, A. Nanayakkara, C. Gonzalez, M. Challacombe, P. M. W. Gill, B. Johnson, W. Chen, M. W. Wong, J. L. Andres, C. Gonzalez, M. Head-Gordon, E. S. Replogle, J. A. Pople, Gaussian, Inc., Pittsburgh PA, **2003**.
- [65] A. D. Becke, *J. Chem. Phys.* **1993**, *98*, 5648.
- [66] C. T. Lee, W. T. Yang, R. G. Parr, *Phys. Rev. B* **1988**, *37*, 785.
- [67] P. J. Hay, W. R. Wadt, *J. Chem. Phys.* **1985**, *82*, 299.

- [68] C. E. Check, T. O. Faust, J. M. Bailey, B. J. Wright, T. M. Gilbert, L. S. Sunderlin, *J. Phys. Chem. A* **2001**, *105*, 8111.
- [69] M. Cossi, G. Scalmani, N. Rega, V. Barone, *J. Chem. Phys.* **2002**, *117*, 43.
- [70] J. Tomasi, B. Mennucci, R. Cammi, *Chem. Rev.* **2005**, *105*, 2999.
- [71] J. Cooper, T. Ziegler, *Inorg. Chem.* **2002**, *41*, 6614.
- [72] S. Sakaki, T. Takayama, M. Sumimoto, M. Sugimoto, *J. Am. Chem. Soc.* **2004**, *126*, 3332.
- [73] F. P. Rotzinger, *Chem. Rev.* **2005**, *105*, 2003.
- [74] B. O. Leung, D. L. Reidl, D. A. Armstrong, A. Rauk, *J. Phys. Chem. A* **2004**, *108*, 2720.
- [75] D. Ardura, R. Lopez, T. L. Sordo, *J. Phys. Chem. B* **2005**, *109*, 23618.

Received: November 26, 2008  
Published online: March 16, 2009